

# Typology of oases in northern Oman based on Landsat and SRTM imagery and geological survey data

Eike Luedeling\*, Andreas Buerkert

*Organic Plant Production and Agroecosystems Research in the Tropics and Subtropics, University of Kassel, Steinstr. 19,  
D-37213 Witzenhausen, Germany*

Received 23 February 2007; received in revised form 29 July 2007; accepted 4 August 2007

## Abstract

In the desert country of Oman, available water resources are scarce and scattered. In most locations where water can be accessed, this resource is harnessed by oases planted to date palm (*Phoenix dactylifera* L.) and other crops. So far, little is known about the site-specific conditions determining the existence, size and type of these oases. Remote sensing and image processing techniques were used to locate oases, to characterize the sites according to their topographic, hydrologic and geologic characteristics and to develop a typology of oases in northern Oman.

To derive oasis positions, we calculated the Normalized Difference Vegetation Index (NDVI) of Landsat images covering all of northern Oman, subtracted a regional average NDVI, averaged the resulting grid over  $3 \times 3$  pixels and extracted the brightest of five classes determined by a natural breaks algorithm. A buffer of six pixels was added to the oases and the vegetated area as determined by the NDVI was summarized for these polygons. The oasis detection procedure was validated using Google Earth Pro®. Topographic information was derived from data of the Shuttle Radar Topography Mission (SRTM), complemented by digitized Russian military maps, from which mean elevations and elevation range above the oases within a buffer of 2 km were extracted.

Water contributing upslope area and distance to streams with catchments of 10 km<sup>2</sup> and 100 km<sup>2</sup> were derived from the same elevation model. All geologic formations of northern Oman were assigned to one of 7 groups and tested for influence on vegetation surrounding them. Four such geologic settings were identified and described by categorical variables. All input parameters were used to define oasis types based on cluster analysis.

Our algorithm detected 2663 oases in northern Oman, of which 2428 had vegetated areas of more than 0.4 ha, the minimum size for reliable detection. The oases were subdivided into six groups. ‘Plain Oases’ (49% of all oases) lie mostly in the plains east and west of the mountains, and are fed by groundwater flow in Quaternary sediments. ‘Foothill Oases’ (46%) are scattered over the foothills, where they draw their water from groundwater flow that is channeled by rock formations. ‘Mountain Oases’ (3%) and ‘Kawr Oases’ (0.5%) lie in the mountains, close to an unconform boundary between limestones and confining rocks. ‘Drainage Oases’ (0.3%) are the largest oases in northern Oman. They lie close to a drainage channel, which drains the entire area west of the mountains. Finally, ‘Urban Oases’ (1.7%) consist of parks and sporting facilities, which do not lie in conclusive hydrologic settings.

© 2007 Elsevier Inc. All rights reserved.

**Keywords:** Geology; Hydrology; Landsat imagery; Normalized Difference Vegetation Index (NDVI); Oasis agriculture; Shuttle Radar Topography Mission (SRTM)

## 1. Introduction

The major part of the Sultanate of Oman is made up of arid to hyperarid desert, and only a very small portion of the country is covered by more than xerophytic vegetation. Locally, however,

water is concentrated in special geologic or topographic settings, where farmers have been harnessing this scarce resource for thousands of years by channeling surface flow, tapping springs or draining water-soaked subsoil (Costa, 1983). Once made accessible, the water is conducted through intricate systems of irrigation channels to leveled fields, which often lie at considerable distances from the water source.

Most traditional irrigation systems, once established, operate on gravitational flow, without external energy inputs, except for

\* Corresponding author. Tel.: +49 5542 981229; fax: +49 5542 981230.

E-mail addresses: [tropcrops@uni-kassel.de](mailto:tropcrops@uni-kassel.de) (E. Luedeling),  
[buerkert@uni-kassel.de](mailto:buerkert@uni-kassel.de) (A. Buerkert).

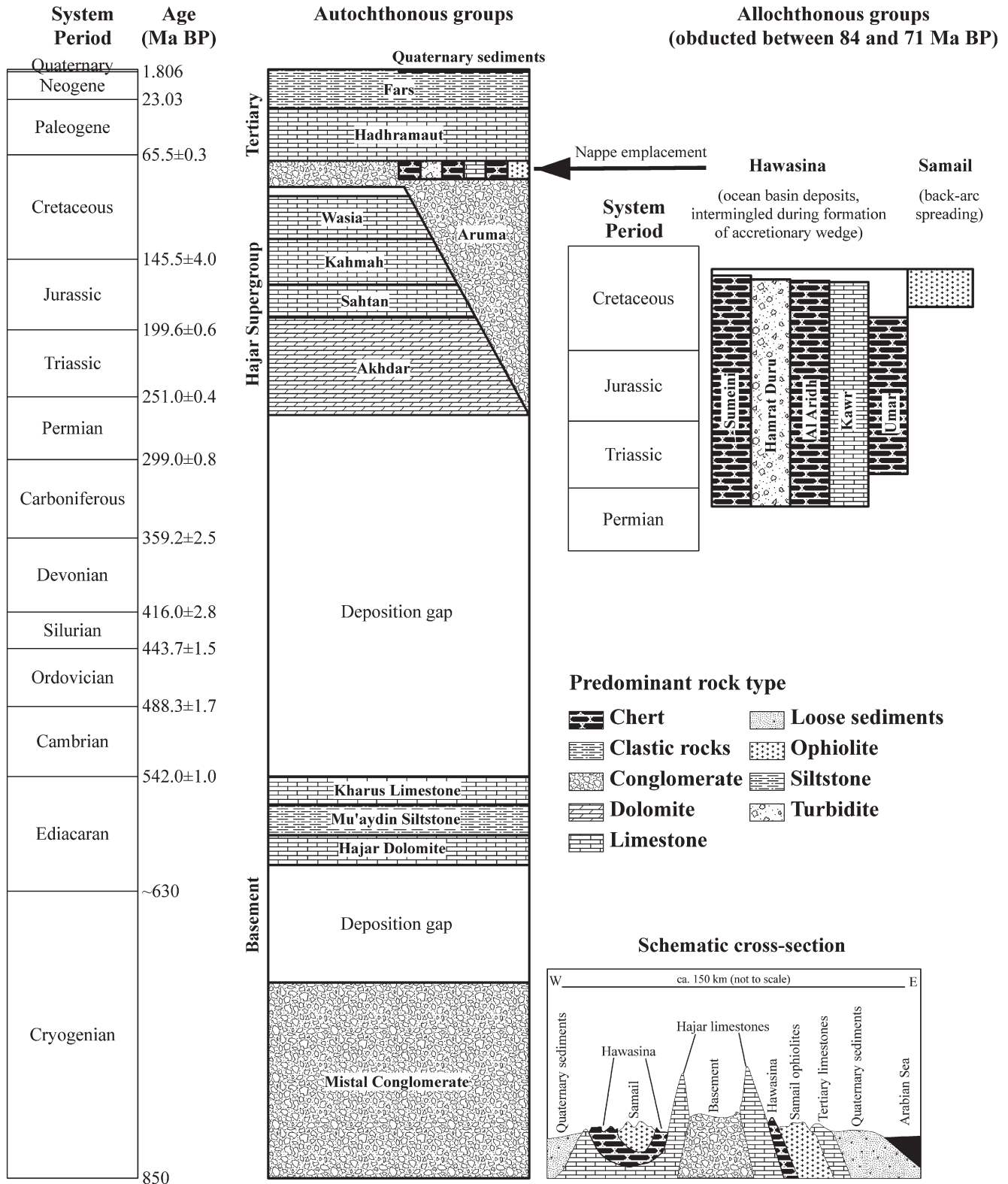


Fig. 1. Simplified stratigraphy and cross-section of the Oman Mountains showing the main geologic groups (Glennie, 2005; Rabus et al., 2003). Numerical ages are according to Gradstein et al. (2004).

some systems on the Batinah coastal plain, which traditionally used water-lifting techniques based on animal traction. Today, this latter method of water acquisition has been replaced by modern electric or diesel-powered pumping systems (Norman

et al., 2001), which now irrigate extensive areas along the coast (Harris, 2003). The modern methods quickly led to overuse of water and created problems of aquifer recession, intrusion of salt water into freshwater aquifers and widespread soil

salinization on the coastal plain (Cookson & Lepiece, 2001). The problems connected with modern pumping techniques make the traditional agricultural systems all the more remarkable, because they managed to survive without evident signs of soil degradation for hundreds or even thousands of years (Siebert et al., 2005). Unlike modern well-based agriculture, these traditional systems could only arise where water could be made accessible using the technologies available at the time of oasis formation. In recent years, these systems have received considerable attention, shedding some light on the factors that ensured the sustainability of oasis agriculture in northern Oman (Gebauer et al., 2007; Luedeling et al., 2005; Siebert et al., 2005; Wichern et al., 2004).

To date, however, no systematic studies have been conducted on the factors that allowed oases to form in the first place. Oases are not randomly distributed over the countryside and their existence is likely to reflect specific hydrologic, topographic or geologic conditions. We hypothesized that oasis locations in Oman can be attributed to a limited number of specific geologic, hydrologic or topographic settings, explainable by proximity to geologic units and topographic features, as well as hydrologic catchment sizes and proximity to intermittent streams, where surface or sub-surface water accumulates. We further hypothesized that it is possible to classify oases accordingly using remote sensing techniques and spatial data processing. The objective of this study therefore was to use such techniques to determine the locations of oases with year-round cultivation in Oman and to develop an oasis typology based on topographic, hydrologic and geologic parameters.

### 1.1. *Geology of the Oman Mountains*

The geology of northern Oman is very complex (Glennie, 2005; Glennie et al., 1974) and some basic information is necessary to understand the effects that geologic setting may have on oasis formation. The following therefore provides a short overview of the mountains' genesis, explaining the origins of the main geologic units represented in the complex stratigraphic column of the mountains (Fig. 1).

Between the Late Permian (260–251 million years before present, Ma BP) and the end of the Early Cretaceous (100 Ma BP), the area that is now Oman was covered by a warm shallow sea, which deposited thick limestone sediments, known as the Hajar Supergroup (Robertson & Searle, 1990). The Hajar unit overlays a basement of Pre-Middle Permian age (before 271 Ma BP), which consists of several types of crystalline rocks and ancient sediments (Gass et al., 1990).

In the Campanian (Late Cretaceous, 84 to 71 Ma BP), the area that now constitutes northern Oman was subjected to the rare geologic process of obduction, in which a slap of oceanic crust was thrust upon the continent (Glennie, 2005). The remains of the ancient seafloor are called ophiolites. They are present in thick layers east and west of the Oman Mountains, constituting the Samail unit. Along with the ophiolites, the Samail unit transported a large amount of other materials onto the Afro-Arabian Platform. These include sediments from former ocean basins, which were scraped off the seafloor by the

overriding tectonic plate and accumulated in an accretionary wedge on the underside of the Samail layer (Ravaut et al., 1997). There is evidence that an entire microcontinent suffered the same fate and was obducted onto the continental shelf. All these materials are referred to as the Hawasina Series. It is mostly made up of sedimentary rocks, which have been intensely folded and faulted during the translocation process, except for the remains of the obducted microcontinent, which constitute the limestones of the Kawr unit (Fig. 1).

The obduction process ceased by the end of the Mid Late Cretaceous and part of the area was once again covered by a shallow sea, resulting in the deposition of large limestone layers until the Late Paleogene (35 Ma BP). Around 35 Ma BP, the opening of the Red Sea divided the Afro-Arabian Plate, separating Africa from Arabia. The pressure build-up created by this separation was partly relieved by warping the eastern margin of the Arabian Plate upwards, forming the giant anticline that now constitutes the Oman Mountains. The final structure of the range was then determined by erosion processes, which freed some underlying rock formations from the obducted layers, and exposed large areas of Hajar limestones. These fall steeply into a central basin, the bottom of which is made up of Basement rocks.

A cross-section through the mountain range (Fig. 1, bottom right) shows that, starting from the Arabian Sea inland, the first geologic feature is a large plain of Quaternary sediments, known as the Batinah coastal plain. Further inland, it is succeeded by limestones of Maastrichtian and Paleogene origin, which in the southern part of the mountains form a large range that extends all the way to the coast. Behind the limestones, large tracts of Samail ophiolites are exposed, followed by sedimentary rocks of the Hawasina unit. These two formations form series of low weathered hills, which are mostly barren except for some vegetation at topographic lows. Hajar limestones are the next stratigraphic unit. They rise steeply from the surrounding area, forming a barrier that is only disrupted by the outlets of some steeply incised intermittent stream beds. These so-called wadis originate from a large basin of Basement rocks. It is surrounded on all sides by Hajar cliffs, which constitute the highest peaks of the mountain range. To the west of the basin, on the lower end of a long slope of Hajar limestone, lies another region characterized by remains of the obduction process. More Hawasina rocks were deposited on both sides of large outcrops of Samail ophiolites. A low range of Hajar limestones is then followed by extensive plains of Quaternary sediments.

Throughout most of the mountain range, erosion processes did not expose the full sequence of rocks described above. The Musandam Peninsula in the north of the country consists almost entirely of Hajar limestones, and between 23.5° and 25.5°N no outcrops of Hajar or Basement occur, so that the central part of the cross-section is characterized by Samail and Hawasina.

## 2. Area of interest and dataset description

### 2.1. *Study area*

The area of interest comprises the range of the Oman Mountains, at the Eastern tip of the Arabian Peninsula (Fig. 2).

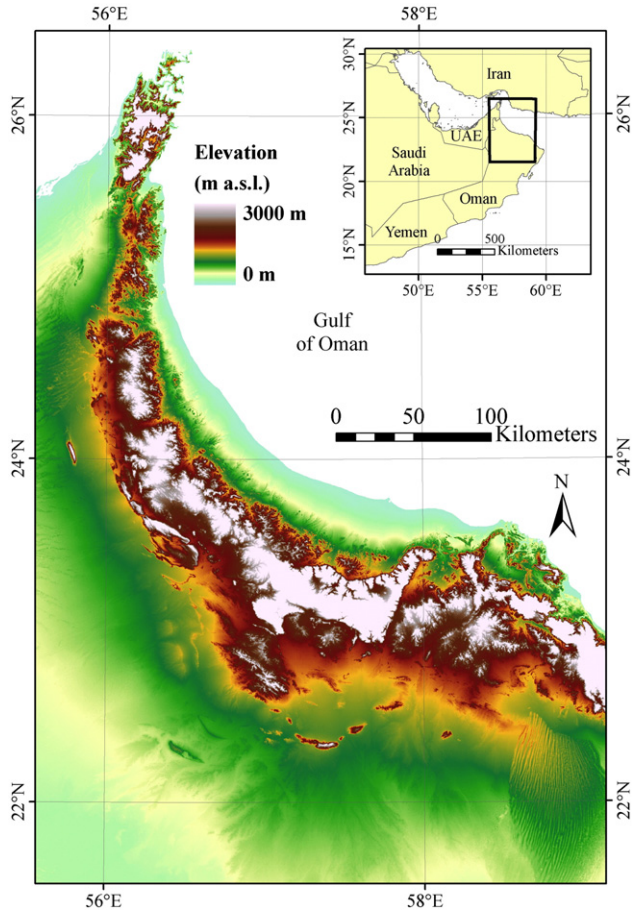


Fig. 2. Location of the study area on the Arabian Peninsula (inset) and topographic map of the Oman Mountain Range.

Within the range, which rises to almost 3000 m a.s.l. at its highest peak, the study was restricted to the national territory of the Sultanate of Oman, because geologic data for the United Arab Emirates were not available. The entire area is characterized by a desert climate with mean annual precipitation ranging from 75 mm in the lowlands to 300 mm in the higher reaches of the mountains (Fisher, 1994). Mean annual temperatures vary between 18 °C at an elevation of 2000 m a.s.l. and 29 °C at sea level, creating environmental conditions that in most places do not allow for a permanent vegetation cover. Bare rock and gravel dominate the landscape, with densely vegetated patches being scattered and rarely larger than about 0.1 ha.

## 2.2. Vegetation dataset

To determine the positions of oases, we used eleven cloud-free satellite images obtained from the University of Maryland's Global Land Cover Facility (GLCF, 2006). These images were taken by the Enhanced Thematic Mapper Plus instrument (ETM+) of the Landsat 7 satellite between January 2000 and August 2001 and covered the entire range of the Oman Mountains (Table 1). We used ENVI 4.2 (Research Systems, Boulder, CO, USA) to merge all images. To compensate for slight differences in light intensity between the images, we used the program's color balancing function based on the overlapping areas. ArcGIS 9.2 (ESRI,

Redlands, CA, USA) was then used to calculate the Normalized Difference Vegetation Index (NDVI; Tucker & Sellers, 1986) for the resulting mosaic, which had a spatial resolution of 28.5 m. This index was calculated using the Red ( $R$ ) and Near Infrared (NIR) bands of the images and deriving the normalized difference as:

$$\text{NDVI} = \frac{\text{NIR} - R}{\text{NIR} + R}$$

## 2.3. Topographic dataset

For analysis of the topography around the oases, we used a Digital Elevation Model (DEM) of the Oman Mountains, which was based on the readings from NASA's Shuttle Radar Topography Mission (SRTM) (Rabus et al., 2003). For areas outside the United States, the spatial resolution of this dataset is 3". Its vertical resolution is 1 m, and for Africa (including Arabia), Rodriguez et al. (2006) determined absolute and relative height errors at 5.6 and 9.8 m, respectively. This satellite-based mission used stereo-imaging to derive surface elevations, which is known to have difficulties in very rugged terrain. These difficulties were reflected in large areas of missing data in the interior of the mountain range. These data voids were filled with elevations derived from topographic maps of the area, which were merged with the SRTM DEM using a delta-surface approach based on Triangular Irregular Networks (TINs; Luedeling et al., 2007).

This elevation model was resampled from its original resolution of 81 m to 85.5 m, which is three times the resolution of the vegetation grid, using a nearest neighbor algorithm (Fig. 2).

## 2.4. Hydrologic dataset

From the same elevation model with a spatial resolution of 85.5 m, we derived hydrologic parameters for the study area using ArcHydro Tools for ArcGIS 9 version 1.1 (ESRI, Redlands, CA, USA). We estimated the flow accumulation in each pixel of the elevation grid by using the standard terrain preprocessing functions to fill sinks, derive flow direction and obtain flow accumulation. For each pixel, the resulting flow accumulation grid contains the number of upslope pixels from the DEM that drain into the pixel. This grid was multiplied by the

Table 1  
List of Landsat ETM+ scenes used in this study

Path	Row	Acquisition date
157	44	19 Sep 2000
	45	23 Jan 2000
158	44, 45	28 Oct 2000
159	42	31 May 2001
	43, 44, 45	31 Jul 2000
160	42, 43	23 Aug 2000
	44	26 Aug 2001

Table 2  
Geologic subdivisions used in the analysis

Name	Stratigraphic units	Rock type	Age
Basement	Basement	Sedimentary, metamorphic and crystalline rocks	Pre-Middle Permian
Hajar	Hajar Supergroup	Limestone	Late Permian to Mid Cretaceous
Non-Hajar limestones	Tertiary limestones and Kawr Group of the Hawasina	Limestone	Tertiary, Late Permian to Mid Cretaceous (Kawr)
Hawasina	Hawasina excluding Kawr Group+Sumeini Group+Aruma Group	Mostly sedimentary rocks	Late Permian to Mid Cretaceous
Samail	Samail+Metamorphic sole+Tertiary listwaenite	Crystalline and metamorphic rocks	Late Cretaceous, Tertiary
Tertiary non-limestones	All tertiary formations excluding limestone	Sedimentary rocks	Tertiary
Quaternary	Quaternary sediments	Uncompacted sediments	Quaternary

size of one pixel ( $85.5 \times 85.5 \text{ m}^2$ ) to obtain the contributing upslope area.

From the flow accumulation grid, we defined two sets of streams using minimum contributing upstream areas of  $10 \text{ km}^2$  (1368 cells) and  $100 \text{ km}^2$  (13,679 cells) as stream definition

thresholds. These two catchment sizes are meant to represent dependence on small local and large regional drainage networks. We use the term “stream” as an analogue to the terminology used in the ArcGIS extension. It should be kept in mind, however, that there are no permanent streams in the

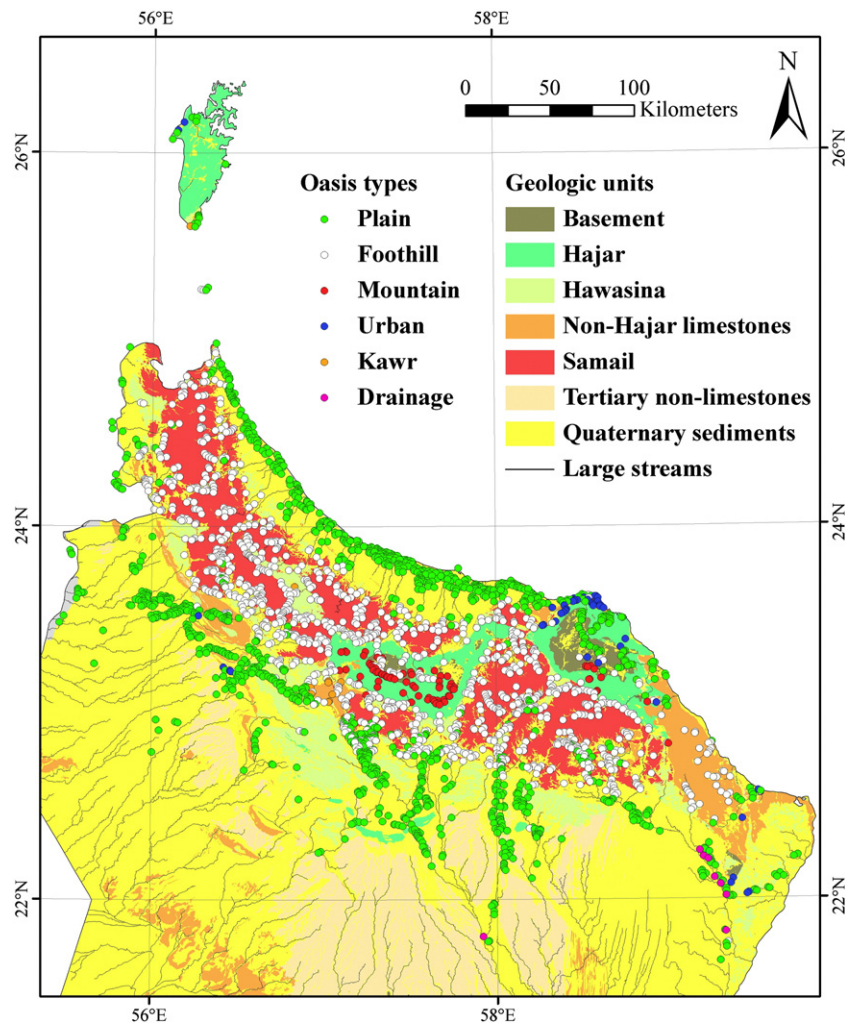


Fig. 3. Geologic groups of northern Oman, according to the classification used in this study, and locations of oases determined by cluster analysis. Lines in the map indicate the locations of streams fed by catchments of more than  $100 \text{ km}^2$ . For illustration purposes, oasis polygons are represented by their central points.

Oman Mountains, and that the streams delineated by hydrologic modeling correspond to intermittent streams (Arab.: wadi) that only have surface flow after heavy rains.

### 2.5. Geologic dataset

To analyze the oases' geologic settings, we obtained a polygon dataset describing the geology of Oman according to a regional survey at a scale of 1:100,000 conducted by the French Bureau de Recherches Géologiques et Minières (BRGM, Orléans, France; Rabus et al., 2003). We summarized all geologic formations into larger geologic units according to their geologic and hydrologic characteristics. The resulting reclassification (Table 2) was mainly aligned with the stratigraphic subdivisions of the mountain range (Fig. 1). For the Basement, the Hajar Supergroup and the Quaternary sediments, the entire stratigraphic units were treated as one group in the analysis. All limestones not belonging to the Hajar Supergroup were agglomerated in a separate group, regardless of whether they were of Tertiary origin or part of the Kawr Group, which belongs to the Hawasina thrust sheet. This classification seemed more appropriate than treating the entire Hawasina as one unit, since limestone was expected to have a different hydrologic behavior than the sedimentary rock types that constitute the rest of the Hawasina. The remaining Hawasina formations were aggregated with the Early Cretaceous Sumeini and Late Cretaceous Aruma Groups. Even though the hydrologic properties of these formations might differ somewhat, they are expected to behave rather as confining than as water-storing units.

The Samail Nappe was aggregated with the associated Metamorphic Sole and with the Tertiary listwaenite, since all three geologic units constitute compact rock types with low water storage capacity, and can be expected to act as barriers to surface and groundwater flow. All Tertiary formations except the Tertiary limestones were aggregated in a separate group.

The reclassified polygon feature was converted into a 85.5-m grid using the ArcGIS 9.2 standard conversion function, which assigns values to pixels based on the polygon that covers the central point of each pixel (Fig. 3).

## 3. Methods

### 3.1. NDVI image enhancement

In spite of the color balancing, some variation in light intensity remained, because the images were taken during different seasons and showed areas at different elevations. Images taken during the hot summer months had much lower overall NDVI ranges than images taken during winter. Similarly, relatively abundant rainfall in the higher reaches of the Oman Mountains provided for more natural vegetation than in the lowlands. Since evapotranspiration in the high mountains is also much lower than in the lowlands, both oases and natural vegetation in the mountains had higher NDVI values than their lowland counterparts. Some lowland oases on summer images therefore had lower NDVI values than natural vegetation in the

mountains on a winter image and prevented using a single threshold to isolate oases. Since everywhere in northern Oman the perennial date palm orchards are well watered throughout the year, we hypothesize that their photosynthetic activity should be much higher than that of the surrounding natural vegetation. Therefore, subtracting a regional background from the NDVI grid before applying the thresholding technique should compensate for the seasonal and altitudinal differences. Bilinear interpolation was used to resample the NDVI grid to 85.5 m resolution and to calculate the regional background NDVI using focal statistics on an area of  $101 \times 101$  pixels (corresponding to  $303 \times 303$  pixels of the NDVI grid). This entailed using a moving window to focus on each pixel of the grid and replacing the value of the pixel by the mean NDVI computed from the  $101 \times 101$  neighboring pixels. This background value was then subtracted from the original NDVI mosaic, making local NDVI maxima stand out more clearly. This grid, which retained the original NDVI resolution of 28.5 m, will be referred to as the enhanced NDVI and allows better distinction between natural and oasis vegetation.

### 3.2. Exclusion of natural vegetation

Finally, it was necessary to exclude natural vegetation from the classification. In contrast to oases, intense natural vegetation typically occurs in very small patches of less than three pixels, whereas most oases are much larger. We therefore applied focal statistics to the enhanced NDVI grid, computing mean values of  $3 \times 3$  pixels centered on each pixel of the grid. This step de-emphasized vegetation clusters of only one or few pixels. The resulting grid was then classified into five classes using a natural breaks algorithm, which ordered all values of the grid and created the class boundaries at natural jumps in the values, and the highest class was interpreted as delineating oasis cores.

In order to estimate how far the oases extended beyond the delineated core, we created ten buffers in increments of one pixel around the oasis cores and calculated the mean of the enhanced NDVI grid for each buffer. This analysis showed that mean NDVI was positive within a buffer of six pixels around the oasis cores (Fig. 4). We therefore accepted a six-pixel buffer as delineating oasis areas.

In order to estimate the vegetated area of each detected oasis, we classified the enhanced NDVI grid into five classes using

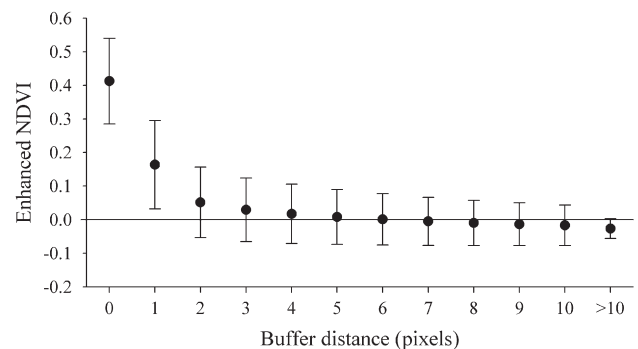


Fig. 4. Mean enhanced NDVI within increasing buffer distances around the oasis cores. Error bars indicate  $\pm$  one standard deviation.

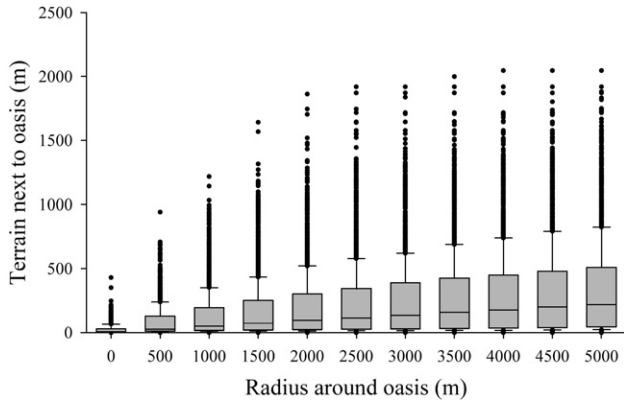


Fig. 5. Terrain next to oases within increasing radii around the oases, calculated as the difference between the maximum elevation within the given radius and the mean elevation of the oasis.

again the natural breaks procedure mentioned above. The highest class was interpreted as vegetated. The result of this classification provided vegetated areas at a higher resolution than the grid used to delineate oasis cores, because the grid had not been subjected to the  $3 \times 3$  pixel focal statistics described earlier in this section. It therefore included both small patches of cultivated vegetation and clusters of dense natural vegetation. We used the six-pixel buffer around the oasis cores to distinguish between the two vegetation types, assuming that vegetation within this buffer belonged to the corresponding oasis. For each oasis polygon, we therefore summarized the area covered by pixels classified as vegetated and used the result to estimate the vegetated area of the oasis.

### 3.3. Classification validation

To test the quality of the classification, we created ten squares of  $20 \times 20$  km<sup>2</sup> and distributed them randomly over the study area. We imported these squares into Google Earth Pro® (Google, Mountain View, CA, USA) and shifted them slightly to overlap with areas of the Google Earth mosaic that were available in high resolution. These parts of the mosaic are based on Quickbird satellite images of submeter resolution. Even though the image resolution in Google Earth might be somewhat lower than in the original Quickbird images, oases were clearly visible, allowing the use of the Google Earth Pro interface for validating the classification. The oasis areas were converted to polygon shapefiles and added to the Google Earth Pro view. We then visually scanned each square for oases, and registered whether the oasis was detected or missed by our algorithm. For those that were missed, we estimated the area of the corresponding palm gardens by using the program's area measuring tool. We also counted the number of polygons that were falsely classified as belonging to an oasis core.

### 3.4. Topographic analysis

Mean elevations of each oasis polygon were then derived using zonal statistics. As an additional topographic variable, we calculated a variable describing the terrain next to each oasis,

which we defined as the difference between the highest point within a given radius around the oasis and its mean elevation. To decide which radius was most appropriate, this parameter was calculated for buffer distances at 500-m increments up to 5 km around the oasis polygons. The variation of elevations next to an oasis rose steeply within 2000 m around the polygons, after which the increases leveled off (Fig. 5). We therefore calculated the terrain next to each oasis as the difference between the highest elevation within a 2-km buffer around each oasis and the mean elevation of the oasis polygon.

### 3.5. Hydrologic analysis

Since many oases do not lie directly in drainage channels, but are likely to be influenced by such channels in their vicinity, flow accumulation within a certain distance from the oases had to be considered. As described in Section 3.4 for the terrain, we constructed buffers of increasing distance around the oases and summarized maximum flow accumulation for each buffer. The result showed that flow accumulation was almost similar for all radii above 2000 m (Fig. 6). We therefore included the value of the pixel with the maximum flow accumulation within a 2-km radius around the oasis as a hydrologic variable.

For each set of streams, we calculated a grid dataset containing the Euclidean distance between each grid point and the nearest stream. From these grids, we chose the minimum distance within each oasis polygon as an input variable.

### 3.6. Geologic analysis

We extracted each geologic class from the grid and calculated the Euclidean distance between each pixel of the study area and the nearest occurrence of each geologic class. We classified these distance grids into zones of increasing distance from the formation, at increments of one kilometer, and calculated the enhanced NDVI for each of these proximity zones (Fig. 7).

The resulting diagrams showed that the only four geologic groups that are directly correlated to the presence of vegetation were Hajar, Hawasina, Samail and Non-Hajar limestones. Moreover, the shape of the NDVI curves indicated that vegetation

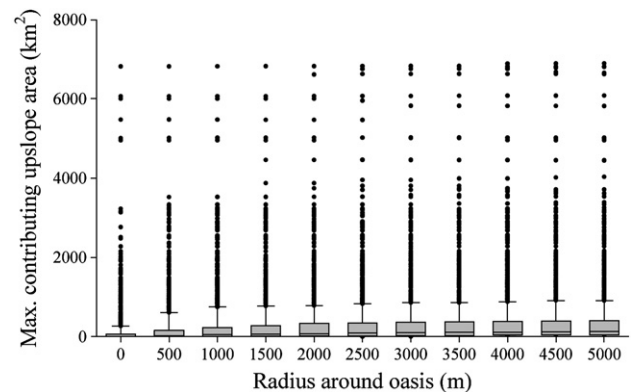


Fig. 6. Maximum contributing upslope area of grid pixels within increasing radii around the oasis polygons.

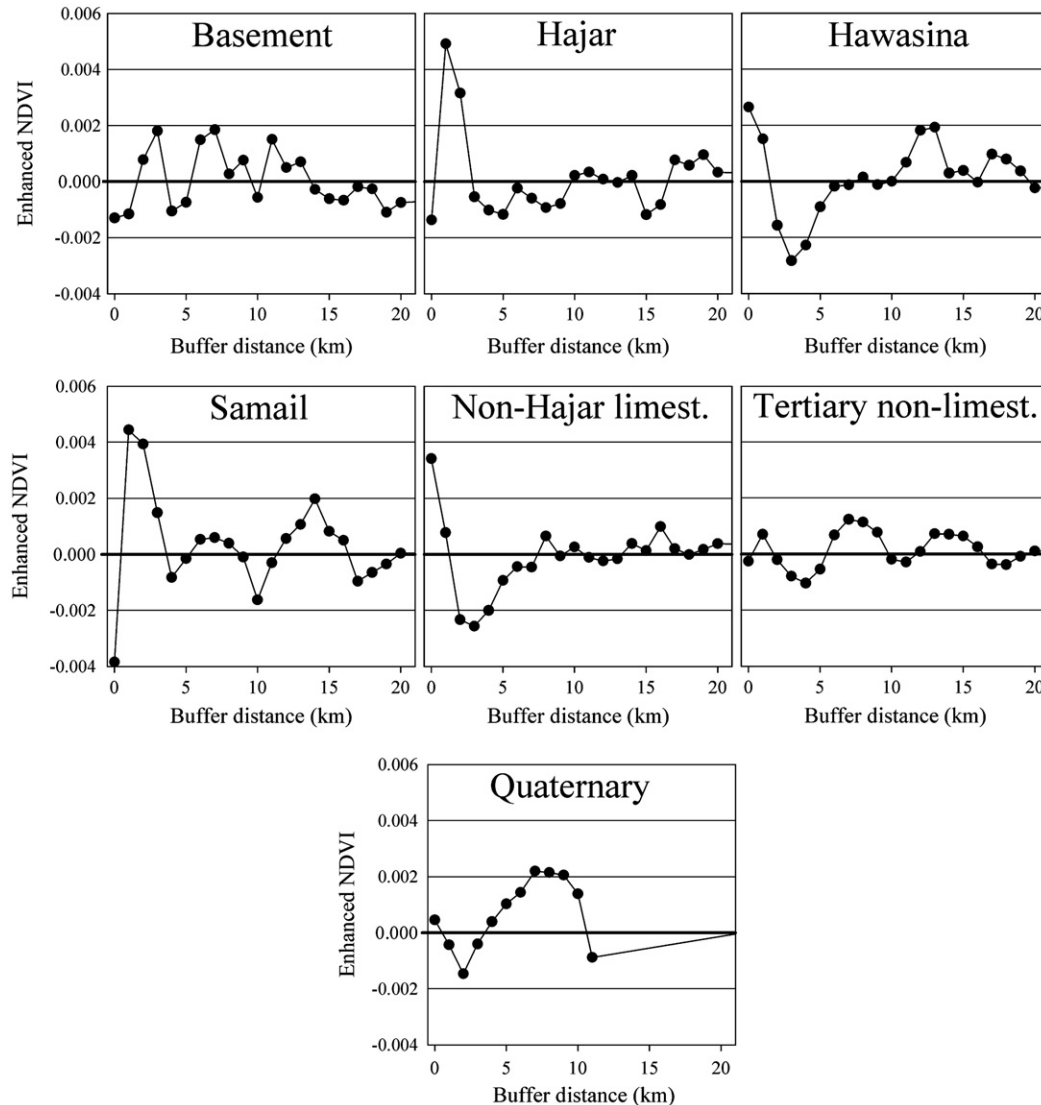


Fig. 7. Mean enhanced NDVI at increasing buffer distances around each of the geologic classes considered in this study.

near these units was different from vegetation on the units themselves. The NDVI curves thus hinted at the boundaries between the respective units and the surrounding rocks as an important factor influencing vegetation. Analysis of the geologic settings of oases thus had to adequately distinguish between oases on these rock units and oases near the geologic boundaries. To achieve this, we created a new variable for each of the four rock groups, assigning a categorical value of 1, if an oasis was on a formation of the group, 0.5 for direct proximity, and 0 if the oasis was further than a certain buffer distance from the nearest occurrence of the geologic group. According to the NDVI diagrams (Fig. 7), the size of the buffer was set to 3 km for Hajar, 2 km for Hawasina and Non-Hajar limestones and 4 km for Samail, reflecting the distance, at which the groups apparently influenced vegetation around them. While these categorical variables were used as inputs for the cluster analysis (Section 3.7), we used the distribution of distances rather than proximity categories to characterize the groups formed by the cluster analysis.

### 3.7. Cluster analysis

Classification of oases was done by hierarchical cluster analysis using PC-ORD 5.0 (MjM Software, Gleneden Beach,

Table 3  
Topographic, hydrologic and geologic parameters used as input variables for the cluster analysis

Input type	Input grid
Topographic	Mean elevation within oasis polygon
	Terrain height within 2 km of oasis (maximum–mean elevation)
Hydrologic	Distance to nearest stream with contributing catchment of 10 km <sup>2</sup>
	Distance to nearest stream with contributing catchment of 100 km <sup>2</sup>
Geologic	Maximum contributing upslope area within 2 km of oasis
	Proximity to nearest occurrence of Hajar <sup>a</sup>
	Proximity to nearest occurrence of Non-Hajar limestones <sup>a</sup>
	Proximity to nearest occurrence of Hawasina <sup>a</sup>
	Proximity to nearest occurrence of Samail <sup>a</sup>

<sup>a</sup> Geologic groups as defined in Table 2, proximity defined as in Section 3.6.

OR, USA). As input data, we used the topographic, hydrologic and geologic variables of all detected oases (Table 3). Hierarchical cluster analysis classifies all input elements based on some measure of the distance between the elements, as determined by the values of all input variables. For measuring this distance, we used a Euclidean distance measure, which calculates the distance  $d_{x,y}$  between two elements  $x$  and  $y$  as:  $d_{x,y} = \sqrt{\sum_i (x_i - y_i)^2}$ , with  $i$  being an index running through all input variables.

Since this distance measure is sensitive to differences in scale among the input variables, giving greater weight to variables with wide ranges, we standardized all topographic and hydrologic input variables by division by the respective maximum value of the variable. To account for the skewed distribution of all variables (Fig. 8), the results were subjected to

square-root transformation. Furthermore, since topography, hydrology and geology were assumed equally important but were represented by different numbers of variables, all variables were weighted by multiplying by factors of six (for the two topographic parameters), four (three hydrologic parameters) and three (four geologic parameters) to assign equal weights to all three categories.

A further parameter in a cluster analysis is the group linkage method, which prescribes how to calculate the distance between clusters of more than one element. For this, we used the unweighted group average method, in which the distances between clusters are calculated from the average distance between all element pairs of the two clusters. The number of clusters was chosen so that the clustering retained just over 4% of the information in the dataset.

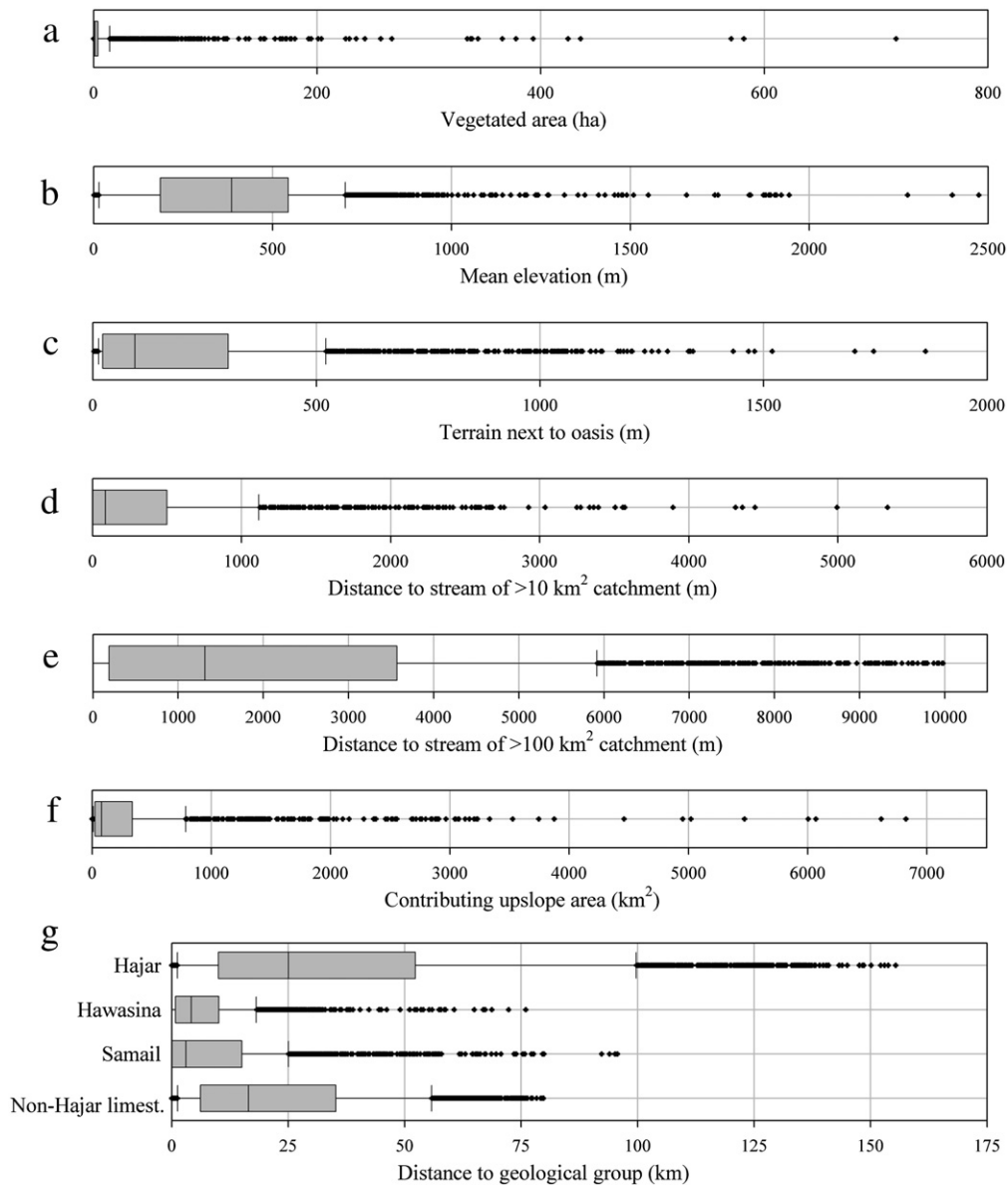


Fig. 8. Overall distributions of all parameters assessed in this study for all 2663 oases detected in northern Oman. In the box plots, the central line represents the median of the dataset, the outer edges of the boxes are the 25% and 75% quantiles, the ends of the error bars represent the 10% and 90% quantiles and the individual points are outliers beyond these limits.

## 4. Results

### 4.1. Oasis locations

Our algorithm detected a total of 2663 oases, ranging in size from 0.08 to 718 ha of vegetated area. Of these 2663 oases, 2428 had vegetated areas of more than 0.4 ha, which was the minimum size for reliable detection (Section 4.2). Among the largest twelve oases, seven were modern agricultural schemes on the Batinah coastal plain. The largest traditional oases were Bilad Bani Bu Hasan (22.07°N, 59.28°E, 436 ha), Al Kamil (22.21°N, 59.21°E, 393 ha), Samail (23.30°N, 57.98°E, 366 ha), Nizwa (22.93°N, 57.53°E, 337 ha) and Rustaq (23.38°N, 57.42°E, 334 ha).

### 4.2. Verification of oasis locations

Comparing the numbers and locations of oases from the classification with the oases that were visible on the Google Earth image within the test areas indicated that the classification was quite accurate (Table 4). Instead of the 156 oases traced visually, the classification found 123 (79%) and only missed 33 (21%). The size of the missed oases ranged between 0.1 and 0.4 ha, compared to an average oasis size of 9 ha. At the Landsat resolution of 28.5 m, such small structures are difficult to distinguish from natural vegetation. In two cases, natural vegetation was interpreted as belonging to an oasis. The first test area, which lay in the Musandam Peninsula, contained several villages, which seemed to depend on rain-fed agriculture and had no palm gardens. Our algorithm did not detect any of these settlements, because the corresponding satellite image was taken during the dry summer. Since our study aimed at describing oases that are located in hydrologic settings that allow year-round cultivation, the failure to detect these locations does not constitute a problem for the analysis. Perennial oases with vegetated areas of more than 0.4 ha were detected correctly in all cases that occurred in the test areas.

Table 4  
Verification of the classification procedure based on Quickbird images in Google Earth Pro®

Test square	Central point	Detected oases		Undetected oases	
		Correct	False	<i>n</i>	Size range (ha)
1	25°56'N; 56°12'E	0	0	0	–
2	22°11'N; 56°40'E	3	0	1	0.2
3	23°36'N; 56°46'E	36	0	12	0.1–0.4
4	23°14'N; 57°04'E	22	1	5	0.1–0.4
5	23°00'N; 57°39'E	14	1	0	–
6	22°44'N; 57°13'E	9	0	1	0.2
7	22°17'N; 56°31'E	0	0	0	–
8	23°24'N; 58°42'E	8	0	6	0.2–0.4
9	22°50'N; 58°42'E	29	0	6	0.1–0.3
10	22°21'N; 59°25'E	2	0	2	0.1
Total		123	2	33	0.1–0.4

For each test square of 20×20 km<sup>2</sup>, the numbers of correctly detected oases (correct), of natural vegetation erroneously classified as oases (false) and of undetected oases are given. For undetected oases, the size range according to Google Earth Pro's measurement tool is also indicated.

### 4.3. Distribution of input parameters

Only few oases stood out with large vegetated areas up to 718 ha, but 50% of all oases had less than 1.3 ha. (Fig. 8a). Mean elevations ranged from 1 to 2474 m a.s.l., with a mean at 390 m a.s.l. (Fig. 8b). The three highest identified oases were small patches of dense juniper vegetation near Jabal Shams (23.24°N, 57.26°E), Oman's highest mountain. The highest actual oasis was the village of Sayq (23.07°N, 57.63°E), at an elevation of 1944 m a.s.l. We identified only 15 other oases above 1500 m a.s.l. Terrain next to the oases was on average 201 m (Fig. 8c). For half of the oases, it was below 94 m, while the maximum was 1862 m for the small mountain village of Al Hawb just south of Jabal Shams. Half of all oases were within 86 m of a stream with a catchment of at least 10 km<sup>2</sup>, while 315 lay more than 1 km away from such streams (Fig. 8d). These were mostly well-based irrigation schemes or mountain oases lying directly at springs. Mean distance to larger streams (>100 km<sup>2</sup> catchment) was 2.1 km, but ranged from 0 to 10.0 km. Half of all oases were less than 1.3 km from such a stream (Fig. 8e). Mean contributing upstream area of the oases was 307 km<sup>2</sup>, with a median of 79 km<sup>2</sup> (Fig. 8f). Catchment sizes of more than 4000 km<sup>2</sup> were only derived for eight vegetated patches around the oases of Bilad Bani Bu Hassan and Al Kamil, the largest natural oases in the region.

Hajar limestones were within 5 km of 18% of all oases, and more than 20 km away from 59%. Since the obducted geologic layers are widespread on both sides of the mountain range, most oases were relatively close to outcrops of Samail (mean distance of 9 km) and Hawasina (7 km). Non-Hajar limestones were on average 22 km from the oases (Fig. 8g).

### 4.4. Cluster description

The cluster analysis classified the oases into six clusters, comprising between 0.3 and 48.5% of all oases (Table 5).

Cluster 1 contains 1291 oases, with vegetated areas ranging from 0.1 to 718 ha (1.1 ha; numbers in parentheses indicate the median of the distributions within the cluster; Fig. 9a). The oases of this cluster are characterized by low to moderate elevations (Fig. 9b) and mostly have low terrain next to them (Fig. 9c). Hydrologically, they lie in diverse settings, with widely varying contributing upslope areas (Fig. 9f) and distances to small and large streams (Fig. 9d and e). Cluster 1 oases are not particularly associated with any geologic groups (Fig. 9g–j).

The 1231 oases of cluster 2 also have widely varying vegetated areas, ranging from 0.2 to 365.7 ha (1.4 ha; Fig. 9a). They lie at higher elevations than cluster 1 oases (Fig. 9b) and have higher terrain around them (261 m; Fig. 9c). Most cluster 2 oases lie very close (0 m; Fig. 9d) to streams fed by catchments of 10 km<sup>2</sup>. Catchment sizes are almost as variable as for cluster 1 (Fig. 9f). Most oases in this cluster are close to Hawasina (2 km; Fig. 9h) and Samail (0 km; Fig. 9i).

Even though the 75 oases belonging to cluster 3 show a smaller variation of their vegetated areas, the median size of oases of this cluster is about the same as for clusters 1 and 2

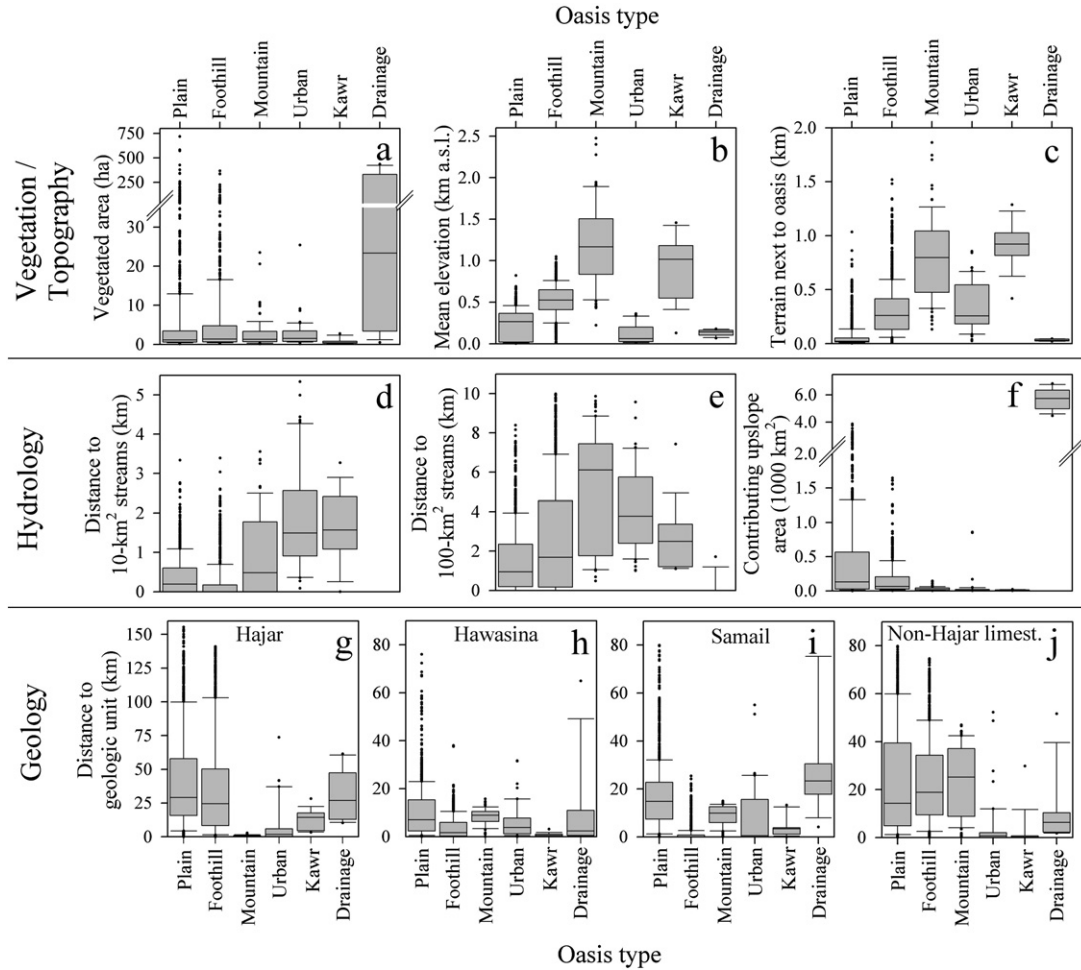


Fig. 9. Distribution of all oasis parameters among the six clusters determined in this study of northern Oman. In the box plots, the central line represents the median of the dataset, the outer edges of the boxes are the 25% and 75% quantiles, the ends of the error bars represent the 10% and 90% quantiles and the individual points are outliers beyond these limits.

(1.3 ha; Fig. 9a). They lie at high elevations (1166 m a.s.l.; Fig. 9b) and have high terrain around them (795 m; Fig. 9c). They are relatively far from small (484 m; Fig. 9d) and large (6.1 km; Fig. 9e) streams, and have small contributing areas (17 km<sup>2</sup>; Fig. 9f). Geologically, they are closely associated with Hajar rocks (0 km; Fig. 9g). In addition to the geologic units that were identified as particularly influential, oases of this cluster were closely associated with Basement rocks (0 km).

The 46 oases of cluster 4 lie at low elevations (Fig. 9a) and are associated with fairly low surrounding terrain (257 m; Fig. 9c). They are far from small and large streams (Fig. 9d and e) and have small catchments (Fig. 9f). These oases are close to Non-Hajar limestones (Fig. 9j).

The 12 oases belonging to cluster 5 are the smallest (0.4 ha; Fig. 9a). They lie at higher elevations than cluster 4 oases (1017 m a.s.l.; Fig. 9b) and have the highest terrain next to them (919 m; Fig. 9c). They are far away from streams and have very small catchment sizes (7 km<sup>2</sup>; Fig. 9f). Cluster 5 oases occur in association with Hawasina (Fig. 9h), Samail (Fig. 9i) and Non-Hajar limestones (Fig. 9j).

Finally, the 8 oases of cluster 6 are the largest (23.4 ha; Fig. 9a), and all have low terrain around them (Fig. 9c). They are strongly

associated with small and large streams (Fig. 9d and e) and draw their water from very large contributing areas (5737 km<sup>2</sup>; Fig. 9f). They are not associated with any geologic group.

Table 5

Results of the cluster analysis for the 2663 detected oases in northern Oman, including oasis types, share of oases in each cluster and general topographic, hydrologic and geologic setting of each type, as interpreted from cluster properties (Fig. 9) and geographic distribution (Fig. 3)

Cluster no.	Oasis type	Share of all oases (%)	Topographic setting	Hydrologic setting	Geologic setting
1	Plain	48.5	Low, flat	Close to streams	–
2	Foothill	46.2	Medium, hilly	Close to streams	Samail, Hawasina
3	Mountain	2.8	High, steep	Natural springs	Hajar
4	Urban	1.7	–	–	–
5	Kawr	0.5	High, steep	Natural springs	Tert. limestones
6	Drainage	0.3	Low, flat	Close to streams	–

A dash (–) indicates that a parameter category (Topography, Hydrology or Geology) was apparently unimportant for the respective oasis type.

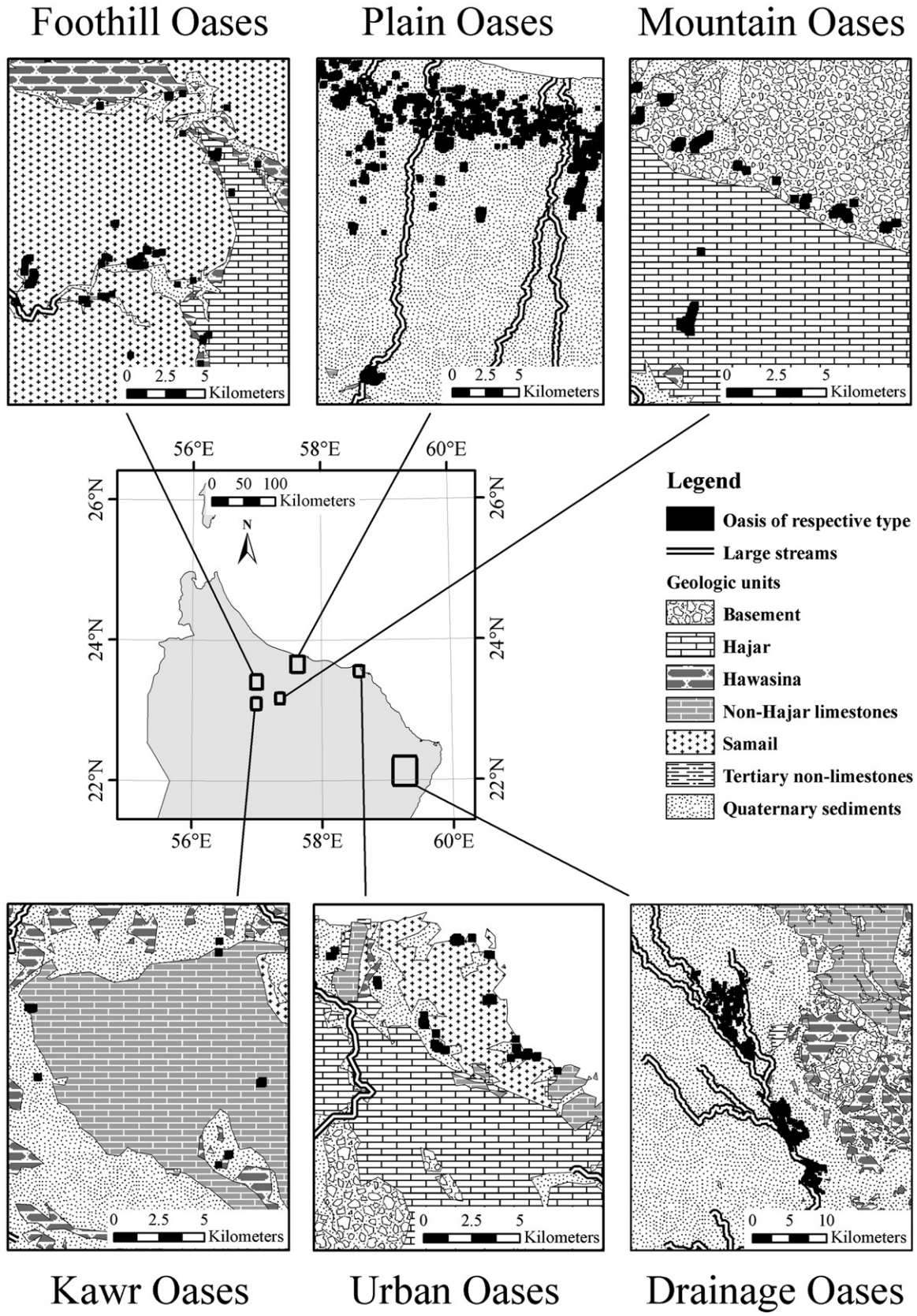


Fig. 10. Geologic setting of the six oasis types in the Oman Mountains.

## 5. Discussion

### 5.1. Cluster characterization

The analysis showed that oases in the Oman Mountains can be found in a wide range of geologic, topographic and hydrologic settings, and that they can be grouped into six distinct categories (Fig. 3, Table 5).

Oases belonging to cluster 1 may be characterized as ‘Plain Oases’, since most of them lie in flat areas at low elevations east or west of the mountains. Virtually all oases of the Batinah coastal plain and most oases on the plain west of the mountains were assigned to this cluster. The elevation range of these oases (Fig. 9b) reflects the different elevations of these two flat areas. These oases are not associated with any geologic settings except for Quaternary sediments (Fig. 10). This indicates that the agriculture of this oasis type is not fed by springs, but either by underground wadi flow, which is tapped by branching off side channels from wadis, or by wells dug into the sediments. This cluster thus mainly comprises the modern irrigation schemes, which are not located where water was easily available in the past, but where groundwater could be accessed by pumps.

Oases of cluster 2, the ‘Foothill Oases’, are scattered over the outcrops of Hawasina and Samail on both sides of the mountains. The oases of this second large cluster lie at higher elevations than ‘Plain Oases’, close to higher terrain and closer to small streams (Fig. 9c and d). They therefore seem to lie in locations, where water is concentrated by local catchments and used to irrigate small palm gardens in valleys of the Hawasina and Samail foothill ranges (Fig. 10). Most such oases appear to be fed by wadi groundwaters rather than by springs, even though some spring-fed oases in comparable geologic settings might also be contained in this cluster.

Oases of cluster 3 are typical ‘Mountain Oases’, lie at high elevation and are mostly in mountainous terrain. While some of these locations might also have some flow accumulation in wadi sediments, the very small catchment sizes and long distances to streams indicate that most oases in this cluster are located close to springs emerging from the geologic unconformity between Hajar and Basement (Fig. 9g). The Hajar limestones form the water storage rocks for these oases, and the Basement is the confining layer that makes the water surface. This unconformity is exposed at various locations throughout the inner mountains, mainly at the upper end of all wadis that penetrate the walls of the central basin and at the edge of the Sayq Plateau in Al Jabal al Akhdar. In all these locations, oases are located near springs emerging from the unconformity setting (Fig. 10).

Oases of cluster 4, the ‘Urban Oases’, are predominantly located in the urban areas of Muscat and Sur and consist of parks, lawn areas and soccer grounds (Fig. 10). Long distances from all streams and small catchment sizes combined with low elevation and flat terrain characterize this cluster (Fig. 9b and c), and suggest that these oases have no natural water supply. In planning sports facilities and parks, considerations about the water supply are generally not the primary concern, and consequently the parameters of this cluster do not represent any

meaningful hydrologic settings. Some agricultural areas are also included in this cluster, but their grouping with the urban areas seems coincidental.

Like these ‘Urban Oases’, the twelve oases of cluster 5 are also associated with Non-Hajar limestones, but their hydrologic setting is more conclusive. They are also associated with Samail ophiolites and Hawasina (Fig. 9h and i), which presumably act as confining layers for an aquifer in the limestones of the Kawr group, around which 10 of the 12 oases in this cluster are grouped. These oases have very small catchment sizes and are far from streams, but the proximity to limestones and the mountainous terrain in the neighborhood indicate that they are fed by springs emerging from the limestones. Based on the locations of these oases close to the limestones of Jabal Kawr, we classify them as ‘Kawr Oases’ (Fig. 10).

The last cluster, the ‘Drainage Oases’ are characterized by the largest catchments of all oases in the mountain range and their locations directly at large streams. Except for outliers of clusters 1 and 2, they are also by far the largest oases in this study. These oases are located to the south–west of the mountain range, in a valley between the mountains and the extensive dune fields of the Wahiba Sands. Based purely on surface topography, this valley drains the entire area west of the mountains, channeling all water flowing towards the sea. Groundwater resources in this location should thus be very large. The settlements of Bilad Bani Bu Hasan and Al Kamil are consequently the largest natural oases in northern Oman.

### 5.2. Factors determining oasis locations

Almost all oases are located close to Quaternary sediments. According to our classification, no oasis lies more than 10 km away from such sediments (data not shown). This is not surprising, because sediments are a necessary prerequisite for oasis formation. In Oman, cultivable soil is often as scarce as water, and it is only available where sediments accumulate or can be accumulated artificially. Even at the oases, which are far from major deposits of such sediments, farmers cultivate fields on sediment patches that are too small to appear on the 1:100,000 scale geologic map, or they collect sediments from elsewhere and transport them to the locations that are to be cultivated.

Other than close to Quaternary sediments, oases were also found in association with limestones of Kawr and Hajar rocks. These oases are associated with springs that are fed by aquifers in the limestones and emerge at the unconformity at the lower end of these storage formations. Both the Hajar and Kawr limestones rest unconformably on rocks of different types (even though from our analysis it is impossible to say if in places the aquifer extends into the thin Precambrian Kharus Group, which stratigraphically lies below the Hajar Supergroup; Fig. 1). The small catchment areas and the relatively large distances to streams of most oases, which lie close to these formations, indicate that their agriculture is fed by springs rather than flow accumulation in sediments. They can thus be considered geologic rather than topographic oases (Table 5).

Most other oases lie much closer to streams and draw their water from much larger catchments. This is particularly true for

oases of cluster 2 ('Foothill Oases'). Even though these oases are closely associated with Hawasina and Samail, the hydrologic properties identify them as topographic rather than geologic oases (Table 5). The geologic groups in their vicinity act as channeling formations rather than storage formations, making sub-surface wadi run-off flow towards the oases, where it can be made accessible by branching off aflaj from the wadi or by digging wells.

The most spectacular examples of such topographic flow oases are the oases of the 'Drainage' cluster (Table 5). The very high flow accumulations of these oases, as well as the high accumulations near some streams on the Batinah Coast make it likely that underground flow leads large quantities of drainage water into the sea. While locally water resources are over-extracted, leading to the intrusion of saltwater into fresh aquifers, it is not unlikely that close to the main drainage channels, additional water could be extracted.

'Plain Oases' are similar to 'Foothill Oases', in that they rely on groundwater stored in sediments rather than on springs (Table 5). Virtually all oases on the Batinah Coast rely on wells, and the same is true for many oases west of the mountains. In both of these settings, many oases are close to streams, but it still seems as if flow accumulation is the deciding factor for the oases' existence. The low topographic gradient in these mostly flat areas makes any form of water acquisition other than from wells difficult to implement. Proximity to streams might thus just be an indicator of groundwater depth, and thus ease of well-digging, but does not necessarily mean that farmers harvest water from the intermittent streams.

'Urban Oases' are neither close to geologic formations that are likely to be storage rocks, nor in topographically favorable places (Table 5). Their locations are largely determined by city planners rather than by water availability. Parks and sports facilities are often irrigated with recycled urban waste water, water from deep wells, or water that has been transported over long distances. They thus may be located in settings, for which economic considerations would preclude irrigation for agricultural production.

Today, the water flow of all major streams in northern Oman, which are likely to correspond to the main drainage lines detected by our analysis, appears to be buried under thick layers of Quaternary sediments. When sea levels were lower during the Last Glacial Maximum (LGM, ~20 ka BP), however, the places where these streams flow into the sea might have been exposed. They may thus be candidates for the now submerged coastal oases postulated by Faure et al. (2002), which are likely to have existed on the exposed continental shelf during the LGM and during the subsequent deglaciation. At that time, the surface of the Arabian Sea was up to 120 m below current sea level (Rohling et al., 1998; Siddall et al., 2003), and even though the Arabian Peninsula is assumed to have been much drier than today (Weyhenmeyer et al., 2000), the locations where the entire flow accumulation of inland northern Oman flowed into the sea are likely to have contained perennial oases. According to Faure et al. (2002), the mouths of these streams might have been important refuges for plants and animals, including early humans.

## 6. Conclusions

Cluster analysis proved a useful tool for classifying oases in northern Oman, which, if their total vegetated area was >0.4 ha, were reliably detected using Landsat imagery and image processing techniques. Our analysis discovered 2428 oases with areas above this threshold.

Based on their reliance on geologic, topographic and hydrologic parameters, Omani oases can be subdivided into six types. 'Plain Oases', 'Foothill Oases' and 'Drainage Oases' draw their irrigation water from groundwater, the accumulation of which can be explained by their topographic settings. For water acquisition, oases of these types rely on wells or sub-surface flow in wadi sediments. 'Mountain Oases' and 'Kawr Oases', in contrast, rely on springs, which emerge from the boundaries of limestone storage formations and confining layers made up of other materials. 'Urban Oases' mostly do not rely on readily available water resources, and thus are not located in hydrologically conclusive settings.

## Acknowledgements

We are indebted to Stefan Siebert for his helpful advice and to the Deutsche Forschungsgemeinschaft for funding this research (BU1308). We also acknowledge the excellent reviews of two anonymous referees, which greatly improved this paper.

## References

- Cookson, P., & Lepiece, A. (2001). Could date palms ever disappear from the Batinah? Salination of a coastal plain in the Sultanate of Oman. In K. A. Mahdi (Ed.), *Water in the Arabian Peninsula— Problems and policies. Exeter Arab and Islamic studies series*. Reading, UK: Ithaca Press, Garnet Publishing Ltd.
- Costa, P. M. (1983). Notes on traditional hydraulics and agriculture in Oman. *World Archaeology*, 14(3), 273–295.
- Faure, H., Walter, R. C., & Grant, D. R. (2002). The coastal oasis: Ice age springs on emerged continental shelves. *Global and Planetary Change*, 33(1–2), 47–56.
- Fisher, M. (1994). Another look at the variability of desert climates, using examples from Oman. *Global Ecology and Biogeography Letters*, 4(3), 79–87.
- Gass, I., Ries, A., Shackleton, R., & Smewing, J. (1990). Tectonics, geochronology and geochemistry of the Precambrian rocks of Oman. In A. Robertson, M. Searle, & A. Ries (Eds.), *The geology and tectonics of the Oman Region*. London, UK: Geological Society Special Publication 49.
- Gebauer, J., Luedeling, E., Hammer, K., Nagieb, M. and Buerkert, A. (2007). Mountain oases of northern Oman: An environment for evolution and in situ conservation of plant genetic resources. *Genetic Resources and Crop Evolution*, 54(3), 465–481.
- GLCF (2006). Earth Science data interface at the global land cover facility. (Accessed on 15 October 2006 at <http://glcf.umiacs.umd.edu/index.shtml>).
- Glennie, K. (2005). *The geology of the Oman Mountains: An outline of their origin*. Beaconsfield, Bucks, UK: Scientific Press.
- Glennie, K., Boeuf, M., Hughes Clarke, M., Moody-Stuart, M., Pilaar, W., & Reinhardt, B. (1974). Geology of the Oman Mountains. *Verhandelingen Koninklijk Nederlands geologisch mijnbouwkundig Genootschap*, vol. 31. (pp. 1–423).
- Gradstein, F., Ogg, J., & Smith, A. (2004). *A geologic time scale 2004*. Cambridge, UK: Cambridge University Press (589 pp).
- Harris, R. (2003). Remote sensing of agriculture change in Oman. *International Journal of Remote Sensing*, 24(23), 4835–4852.

- Luedeling, E., Nagieb, M., Wichern, F., Brandt, M., Deurer, M., & Buerkert, A. (2005). Drainage, salt leaching and physico-chemical properties of irrigated man-made terrace soils in a mountain oasis of northern Oman. *Geoderma*, 125(3–4), 273–285.
- Luedeling, E., Siebert, S., & Buerkert, A. (2007). Filling the voids in the SRTM Elevation Model— A TIN-based delta surface approach. *ISPRS Journal of Photogrammetry and Remote Sensing*, 64(4), 283–294.
- Norman, W. R., Al-Ghafri, A. S., & Shayya, W. H. (2001). Water-use performance and comparative costs among surface and traditional irrigation systems in northern Oman. In K. A. Mahdi (Ed.), *Water in the Arabian Peninsula— Problems and policies. Exeter Arab and Islamic studies series*. Reading, UK: Ithaca Press, Garnet Publishing Ltd.
- Rabus, B., Eineder, M., Roth, A., & Bamler, R. (2003). The shuttle radar topography mission— A new class of digital elevation models acquired by spaceborne radar. *ISPRS Journal of Photogrammetry and Remote Sensing*, 57(4), 241–262.
- Ravaut, P., Bayer, R., Hassani, R., Rousset, D., & Al Yahya'ey, A. (1997). Structure and evolution of the northern Oman margin: Gravity and seismic constraints over the Zagros–Makran–Oman collision zone. *Tectonophysics*, 279, 253–280.
- Robertson, A., & Searle, M. (1990). The northern Oman Tethyan continental margin: Stratigraphy, structure, concepts and controversies. In A. Robertson, M. Searle, & A. Ries (Eds.), *The geology and tectonics of the Oman Region*. London, UK: Geological Society Special Publication 49.
- Rodriguez, E., Morris, C. S., & Belz, J. E. (2006). A global assessment of the SRTM performance. *Photogrammetric Engineering and Remote Sensing*, 72(3), 249–260.
- Rohling, E. J., Fenton, M., Jorissen, F. J., Bertrand, P., Ganssen, G., & Caulet, J. P. (1998). Magnitudes of sea-level lowstands of the past 500,000 years. *Nature*, 394(6689), 162–165.
- Siddall, M., Rohling, E. J., Almogi-Labin, A., Hemleben, C., Meischner, D., & Schmelzer, I. (2003). Sea-level fluctuations during the last glacial cycle. *Nature*, 423(6942), 853–858.
- Siebert, S., Häser, J., Nagieb, M., Korn, L., & Buerkert, A. (2005). Agricultural, architectural and archaeological evidence for the role and ecological adaptation of a scattered mountain oasis in Oman. *Journal of Arid Environments*, 62(1), 177–197.
- Tucker, C. J., & Sellers, P. J. (1986). Satellite remote-sensing of primary production. *International Journal of Remote Sensing*, 7(11), 1395–1416.
- Weyhenmeyer, C. E., Burns, S. J., Waber, H. N., Aeschbach-Hertig, W., Kipfer, R., & Loosli, H. H. (2000). Cool glacial temperatures and changes in moisture source recorded in Oman groundwaters. *Science*, 287(5454), 842–845.
- Wichern, F., Luedeling, E., Müller, T., Joergensen, R. G., & Buerkert, A. (2004). Field measurements of the CO<sub>2</sub> evolution rate under different crops during an irrigation cycle in a mountain oasis of Oman. *Applied Soil Ecology*, 25(1), 85–91.